

Supplementary Data

The Electrochemistry of Size Dependent Graphene *via* Liquid Phase Exfoliation: Capacitance and Ionic Transport

Varisara Deerattrakul^{a,b}, Wisit Hirunpinyopas^c, Nuttapon Pisitpipathsin^a, Thanit Saisopa^a,
Montree Sawangphruk^d, Chakrit Nualchimplee^a, and Pawin Iamprasertkun^a, *

- a. Department of Applied Physics, Faculty of Sciences and Liberal Arts, Rajamangala University of Technology Isan, Nakhon Ratchasima, 30000, Thailand.
- b. National Nanotechnology Center (NANOTEC), National Science and Technology Development Agency (NSTDA), Pathum Thani, 12120, Thailand
- c. Department of Chemistry, Faculty of Science, Kasetsart University, Bangkok 10900, Thailand.
- d. Department of Chemical and Biomolecular Engineering, School of Energy Science and Engineering, and Centre of Excellence for Energy Storage Technology (CEST), Vidyasirimedhi Institute of Science and Technology, Rayong, 21210, Thailand

*Corresponding author information: E-mail address: pawin.ia@rmuti.ac.th,

ORCID ID: [0000-0001-8950-3330](https://orcid.org/0000-0001-8950-3330)

Keywords: Graphene, Liquid Phase exfoliation, Flake size, Capacitance, Ion transport

Experimental section

Controlling the flake size of exfoliated graphene

The graphene dispersion was prepared according to the liquid phase exfoliation of graphite in N-Methyl-2-pyrrolidone process, as shown in **Figure S1**. Initially, 2.0 g of graphite flakes (99% purity, flake size $\sim 150\ \mu\text{m}$ > 80%, Sigma-Aldrich), and 200 ml of N-Methyl-2-pyrrolidone (NMP, 99% purity, Alfa Aesar) were placed in a 250 ml round bottle flask. The prepared mixtures were sonicated at 37 Hz (80 mW) for 12 hours^{1, 2} in order to obtain the graphene dispersion.

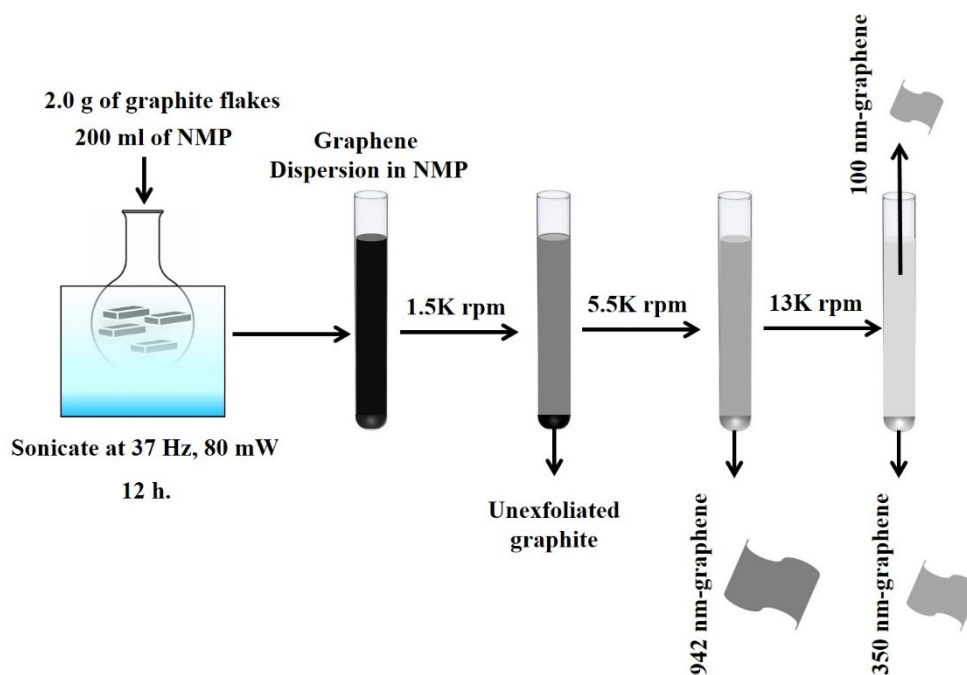


Figure S1: Graphite exfoliation through liquid phase exfoliation and separation of graphene flakes using centrifugation.

In order to control the dimensions of the graphene flakes, the sequent centrifugation method is applied^{3, 4}. Firstly, the graphene dispersion was centrifuged at 1500 rpm for 30 minutes. The supernatant, consisting of a variety of exfoliated graphene flake sizes, was detached from the sediment by removing about 70% of the top layer of graphene

dispersion. Note that this process was repeated twice to ensure that all unexfoliated graphite was removed. Secondly, the taken supernatant from the previous step was then centrifuged at 5500 rpm for 30 minutes in order to obtain large graphene flakes (942 nm-graphene) from the sediment as shown in **Figure S1**. Finally, the top dispersion was again centrifuged at 13,000 rpm for 30 minutes. This left medium graphene flakes (350 nm-graphene) on the bottom as sediment and smaller graphene flakes (100 nm-graphene) in the top dispersion.

Characterisation

Graphene dispersions from the different centrifugal rates were diluted in a solvent of n-propanol and water at the ratio of 1:1 to a concentration of $10\mu\text{g ml}^{-1}$ (total volume 20ml). The graphene flake sizes were then evaluated using the Dynamic Light Scattering (DLS) technique, and the size distribution was presented as a Z-average (the average particle diameter). The zeta potential (E_{zeta}) was measured using a Malvern Nanosizer Z (NIBS) running Zetasizer software. The graphene dispersions were measured in quartz cuvettes (with a 10 mm path length), using an operation in backscatter mode with an angle of 173° with a 633 nm HeNe laser.

To further characterise the surface properties of the prepared samples, the diluted graphene dispersions were then loaded onto the PVDF membrane ($0.1\ \mu\text{m}$ pore diameter, purchased from Millipore Sigma, US) through a syringe pump at an injection rate of $5\ \text{ml h}^{-1}$, and the samples were then dried at 50°C for 24 h. The surface morphology of the prepared graphene samples was characterised by SEM (FEI/Philips XL30 E-SEM, Quanta 650), using an accelerating voltage of 15kV under high vacuum conditions. For TEM measurement, the graphene dispersions were drop-coated onto a copper grid (lacey carbon), and the prepared samples were cleaned with an ion cleaner (EC-520001C, JEOL). The TEM images were obtained from JEM-ARM200F using an accelerating voltage of 200kV. The AFM was carried out using NanoWizard[®] 4 NanoScience AFM (JPK instruments) with a quantitative imaging (QI[™]) mode in air under ambient conditions (Au-coated side of the cantilever, PPP-NCHAuD). AFM images were obtained directly onto the graphene/PVDF support, in which the samples were attached to a glass slide during the experiment using the peak force

setpoint of 30-70 nN. The ImageJ software was applied to evaluate the graphene flake sizes using AFM techniques.

To describe the structural properties of the graphene, a Raman spectra process was performed using a Renishaw inVia Raman microscope with a 532nm laser (an excitation energy of 2.33eV, laser power of 1mW). The XPS was performed by a Kratos Axis Ultra DLD spectrometer using the Al K α (1486.6eV) as an X-ray source. The X-ray diffraction (XRD) was carried out using a PANalytical X'pert X-ray diffractometer with a Cu-K α with a wavelength of 0.154nm as a radiation source operating at 40kV and 30mA.

The wettability of the samples was measured using a Theta Optical Tensiometer (Biolin Scientific, Sweden, running OneAttension software) in a high humidity chamber with a fixed droplet volume of $1.0 \pm 0.1 \mu\text{l}$. This prevents the evaporation of water during measurement.⁵ The images were then recorded at a rate of 26 frames per second. The water contact angle (WCA) was analysed using Young's equation:⁶

$$\gamma_{sv} - \gamma_{sl} - \gamma_{lv} \cos \theta = 0$$

where γ_{sv} , γ_{sl} , and γ_{lv} are solid-vapour, solid-liquid, and liquid-vapour tension respectively.

Electrode preparation

The free-standing graphene electrodes were prepared by filtrating the graphene dispersion (mass concentration $\sim 50 \mu\text{g ml}^{-1}$) onto a PVDF membrane using a syringe pump at an injection rate of 5 ml h^{-1} . The loaded graphene mass was then controlled to $1.3 \pm 0.2 \text{ mg cm}^{-2}$, giving a resultant mass of about 1 mg per electrode. The filtrated electrode was then dried at 50°C for 24 h. In addition, the highly ordered pyrolytic graphite (HOPG) electrode was prepared by it on top of a Si/SiO₂ substrate. The edge of the HOPG was covered with silver and connected with copper wire. The epoxy resin was then applied to the silver and copper parts.

To prepare the Ag/AgCl reference electrode, the silver wire (99.99% purity, Goodfellow Cambridge Limited: GF82496683, 0.20 mm diameter) was immersed in 0.5 M hydrochloric acid. The potential was then applied by chronoamperometry in increments of

0.5V, 1.0V, and 1.5V for 30 minutes using two electrode configurations (platinum wire was used as a counter electrode). The prepared Ag/AgCl electrode was then washed with n-propanol and de-ionized water several times to remove impurities and any residual hydrochloric acid. To prepare an agarose gel, a 3.5 M KCl solution was heated to 80°C. The agarose powder (3% wt.) was then added to the solution and stirred until the gel dissolved. The gel was then carefully poured into the glass body to avoid the air bubbles. The coated Ag/AgCl wire was then placed inside the glass body and filled with 3.5 M KCl electrolyte. Finally, the cap was sealed with the adhesive epoxy resin to prevent any evaporation of the electrolyte from the reference electrode.

Electrochemical setup

The electrochemical setup was divided into three stages based on are two-electrode, three-electrode, and four-electrode configurations as shown in **Figure S2**. For the two electrode configuration, the prepared graphene on the PVDF support was immersed into 0.5 M K_2SO_4 for 30 minutes. The two electrodes (which were of identical mass) were then stacked back to back in the coin cell (CR-2032), and the aluminium spacer and spring were applied in the cell as shown in **Figure S2a**. For the three electrode configuration, the prepared HOPG, Ag/AgCl, and platinum wire were used as a working, counter and reference electrode respectively. The PTFE cell with an opening diameter of 3mm (total exposed area 0.07068 cm^2) was placed on top of the HOPG as shown in **Figure S2b**. The saturated K_2SO_4 (~0.1 ml) was then added into the cell. Note that the HOPG was split before measurement in order to provide a fresh surface. For the four electrode configuration (Ionic conductivity measurement), the prepared graphene on the PVDF support was assembled between two polyethylene terephthalate (PET) sheets as support, with an exposed area of 0.264 cm^2 . This was inserted in a custom-made H-cell beaker consisting of two liquid reservoirs (50 mL) linked with polycrystalline platinum electrodes and prepared Ag/AgCl reference electrodes (see **Figure S2c**). Note that the Ag/AgCl reference electrodes were placed inside Luggin capillaries to eliminate the liquid-junction potential arising from the concentration gradient of the electrolyte. The solutions of the two liquid reservoirs were stirred to minimise the concentration of polarization.³

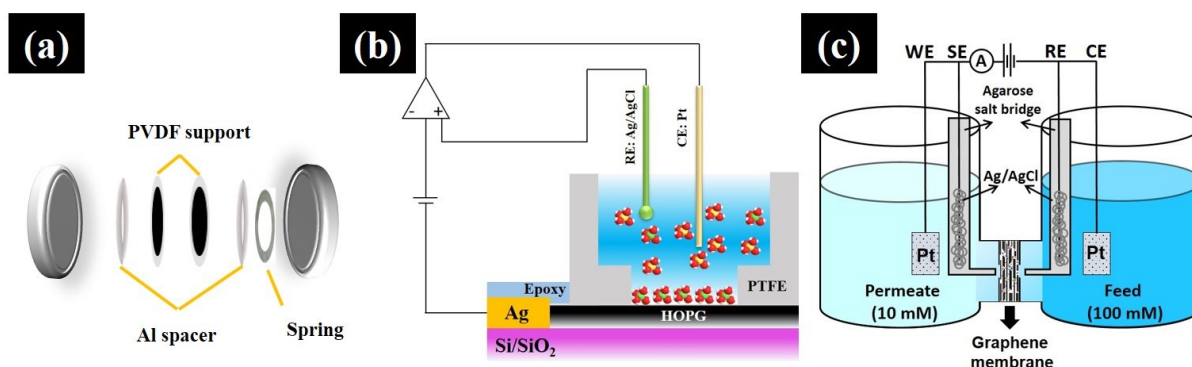


Figure S2: Electrode configurations (a) two-electrodes, (b) three-electrodes, (c) four-electrode measurements.

Electrochemical measurements

For the coin cell measurement, cyclic voltammetry (CV), galvanostatic charge/discharge (GCD), and electrochemical impedance spectroscopy (EIS) techniques were applied using PGStat302N running Nova software version 1.11. To measure the electrochemical properties in each of the graphene flake sizes, the CVs were applied from 10 to 100 mV s^{-1} over a potential window of between 0.0 and 1.0 V. The EIS was tested at the open circuit voltage (OCV) with a 10 mV perturbation from 1 kHz to 100 kHz. For the HOPG measurement (the three electrode system), the EIS was applied over potential window from -0.4 to 0.6 V vs. Ag/AgCl with voltage amplitude of 10 mV from 100 kHz to 1 Hz. In contrast to the two- and three-electrode measurement, the EIS was then applied at a zero current (0 A, galvanostatic technique) to the graphene membrane for the four electrode system from 100 kHz to 0.01 Hz (ionic conductivity measurement).

Electrochemical analysis

The capacitance of graphene was calculated through the integral product of CV using [Equation \(S1\)](#):

$$C_s = 4 \int \frac{idV/v}{m\Delta V} \quad (S1)$$

where m is the mass of graphene loaded onto the electrodes (based on total mass), v is scan rate, and ΔV is the operating potential.

To explore the capacitance of the HOPG using the EIS technique, the interfacial capacitance (C_A) of the HOPG was averaged from a frequency of between 1 Hz and 10 Hz. where the phase approached -90° , showing an ideal capacitor behaviour. The capacitance was calculated using Equation (S2):⁷

$$C_A = \frac{-1}{2\pi f Z'' A} \quad (S2)$$

where f is the applied frequency (Hz), Z'' is the imaginary impedance, and A is the exposed area of the HOPG.

XPS deconvolution

The high resolution XPS spectra were deconvoluted using CasaXPS software. For only C1s spectra, the line shape LA (1, 1.6, 50; for definition, see below) was applied to the sp^2 peak with the FWHM about 0.51 to 0.53. The following carbon peaks C-O, and $\pi-\pi^*$ were then deconvoluted by line shape GL (30) function where the FWHM are about 1.9 to 2.3, and 2.5 to 2.7, respectively. Note, GL (30) is the symmetrical line shape with 70% Gaussian and 30% Lorentzian. LA (1, 1.6, 50) is the asymmetrical Lorentzian line shape at a binding energy above the peak maximum with an exponent of 1.6 in the Lorentzian function.

Results section

Surface topography of graphene samples

Further SEM images in the main text and the TEM images in **Figure S3** show different graphene flake sizes obtained through the liquid phase exfoliation of graphite using the centrifugation method. Obviously, the centrifuged graphene exhibits variety of flake sizes, but it can be seen that the highest centrifugation speed (over 13,000 rpm) provides tiny and thin graphene flakes about 100 nm in size (see **Figure S3a** and **S3b**). As expected, the dimensions of the graphene flakes increase to 200-400 nm when the centrifugation speed is reduced to 5,500 rpm (see **Figure S3c** and **S3d**). Once the centrifugation speed passes 1,500 rpm, the exfoliated graphene in **Figures S3e** and **S3f** displays flakes approximately 1 μm in size. These results show an excellent correlation with other characterisation techniques such as SEM and DLS, as well as previous studies.^{3, 4} To further characterise the flake size distribution of the prepared graphene dispersion, the AFM couple (*via* imageJ) were then applied with image analysis as shown in **Figure S4**. Overall, the flakes size analysed through AFM technique shows similar trend and comparable graphene flake sizes in other characterisation techniques confirm a strong evidence of the graphene flake sizes obtained. The graphene sample centrifuged at 13,000 rpm shows a variety of flake sizes from 20 nm to 270 nm, as shown in **Figure S4b**, with an average flake size of 112 ± 2 nm (N=350). The average flake size increases to 343 ± 5 nm (N=350) when the centrifugation rate is reduced to 5,500 rpm. The flake size distribution was found to be between 150 and 700 nm (see **Figure S4d**). Once the centrifugation rate is decreased to 1,500 rpm, the average flake size increases to 884 ± 11 nm (N=400), while the size distribution is between 400 and 1,600 nm.

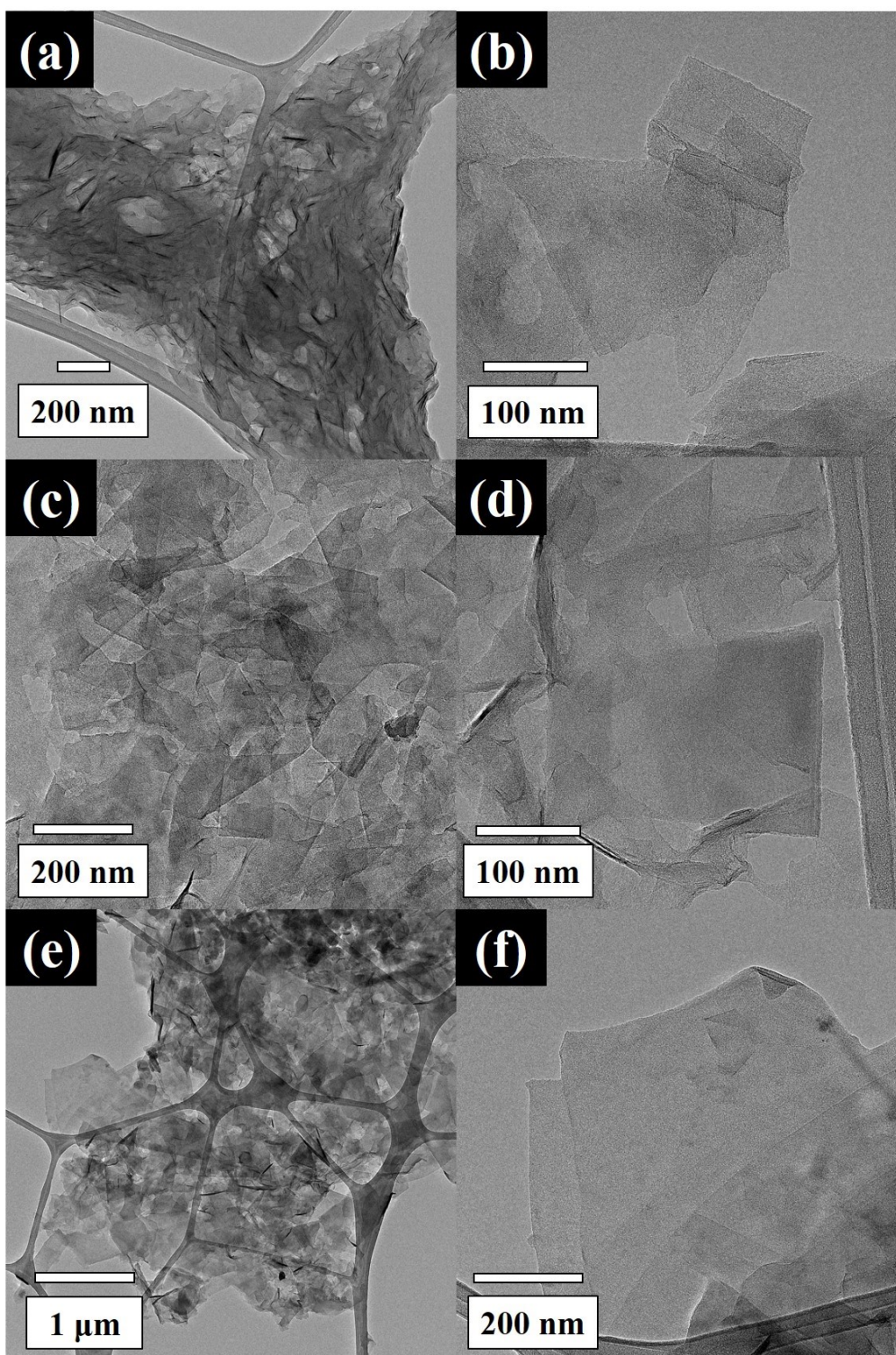


Figure S3: the TEM images of the prepared graphene (a, and b) 100 nm-graphene, (c, and d) 350 nm-graphene, (e, and f) 942 nm-graphene where (a, c, and e) are low magnification images, and (b, d, and f) are high magnification images.

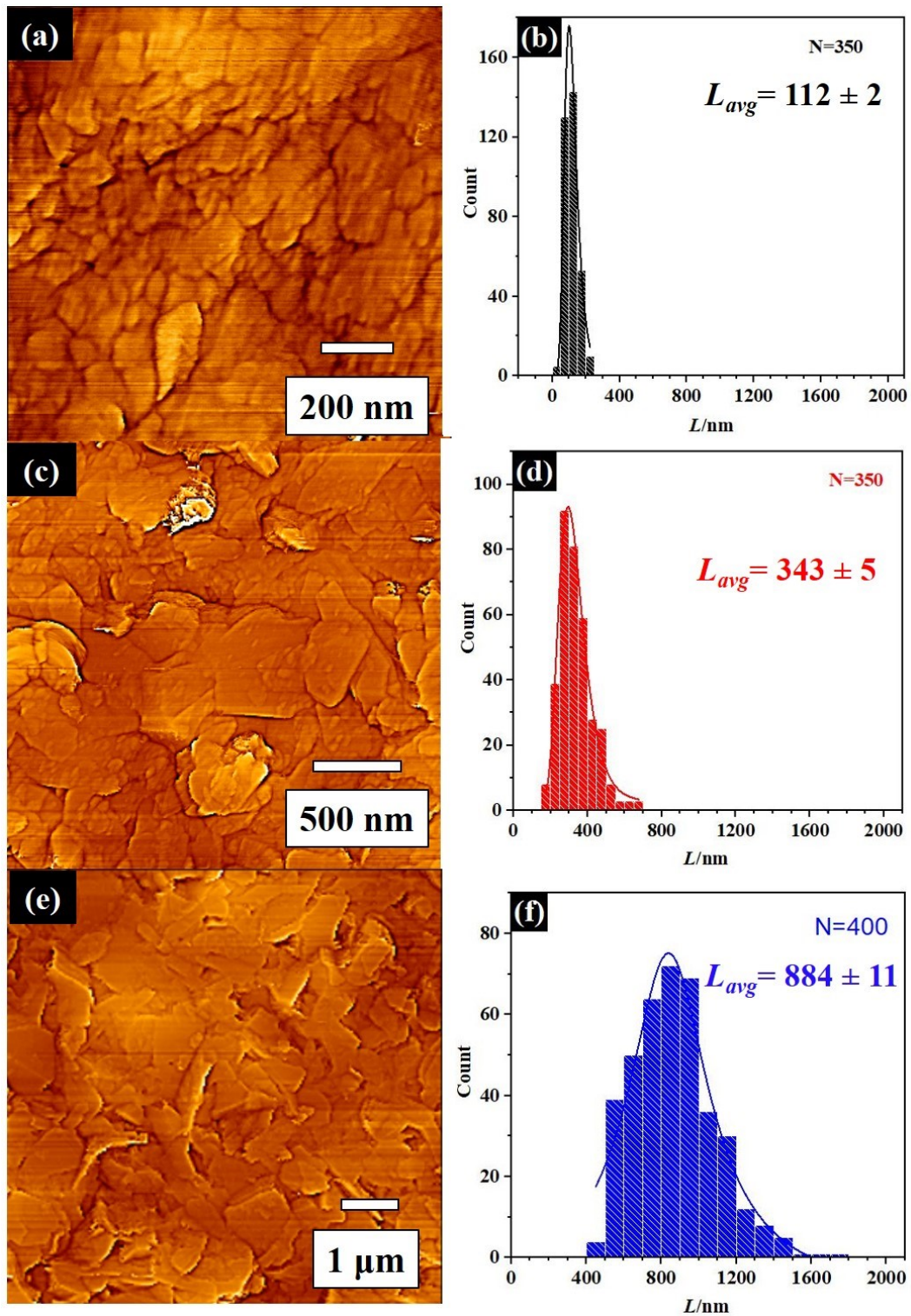


Figure S4: the surface topography of different graphene flake sizes (a, c, and e) and flake size distribution (b, d, and f) where (a, and b) is the 100 nm-graphene, (c, and d) is the 350 nm-graphene, and (e, and f) is the 942 nm-graphene, respectively.

Structural properties of exfoliated graphene

As well as the Raman, the XRD pattern of the prepared samples from graphite to graphene is shown in **Figure S5**. As discussed in the Raman results section, higher centrifugation rates give a smaller dimensions of graphene in terms of both length and thickness. The XRD of graphite flakes in **Figure S5** shows a reflection pattern of (002) plane at about 26.7° , with a graphite d-spacing of 0.335 nm ⁸. It is evident that the (002) plane shifted to the lower angle once the graphite had been exfoliated, indicating the expansion of the interlayer spacing. This is typically observed when performing a liquid phase exfoliation of two dimensional material e.g. graphite-graphene^{9, 10}, transition metal dichalcogenides (TMDs)¹¹, Mxene¹². Clearly, the 942 nm-graphene displays a significant (002) plane shift towards lower degree. This may be assign to the incomplete graphite exfoliation, which leaving the solvent trapped inside the structure. Moreover, the full width half maximum (FWHM) of the exfoliated graphene samples also increased when the graphite turned into to graphene sheets and lower dimension graphene flakes. This confirms that the number of graphene layers reduce when a higher centrifugation rate is applied,¹ a result that agrees with our findings from the Raman spectra.

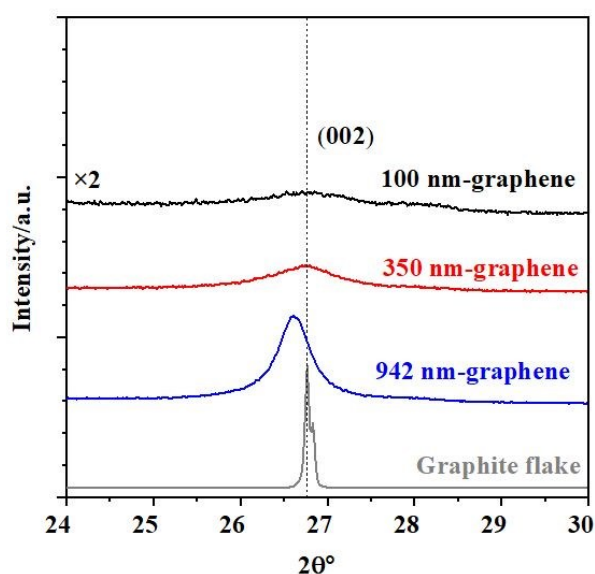


Figure S5: the XRD pattern of the exfoliated graphene from graphene to graphite.

Furthermore, the surface chemical composition of the samples was then analysed using XPS, as shown in **Figure S6**. It is found that the XPS survey spectra in **Figure S6a** showed three

peaks, which are C1s, N1s, and O1s. The carbon content of all the exfoliated samples are over 97%, while the nitrogen and oxygen content is about 2 %, and 1 %, respectively. Note that the nitrogen species on the exfoliated graphene sample originated from the NMP solvent.² When considering the relationship between the carbon and oxygen content, it is evident that the carbon to oxygen ratio (C:O) increases along with flake size, as can be seen in **Figure S6b**. The C:O ratios are about 52, 65, 89, and 115, respectively, when the flake size increases from 100 nm (graphene) to 100 μm (graphite).

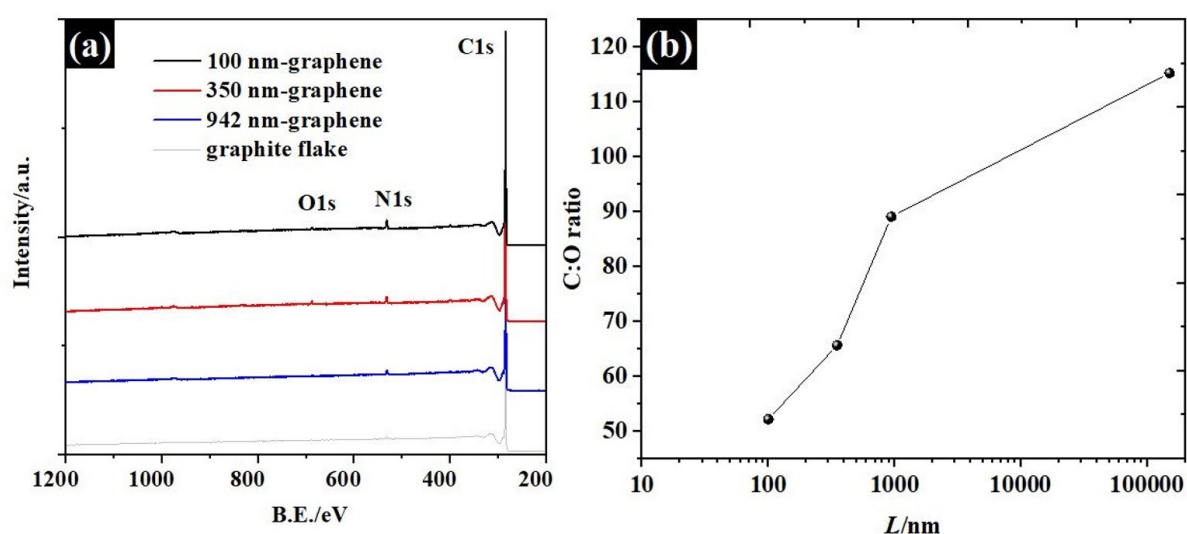


Figure S6: the surface chemical composition of the prepared graphene analysed via XPS (a) XPS survey spectra, and (b) carbon to oxygen ration in respect of the graphene dimension.

Moreover, the analysis of high resolution spectra are shown in **Figure S7**. Obviously, all graphene samples exhibit similar C1s profile, which consist of C-C, C-O, and the π - π^* peaks at about 284.8, 286.5 and 291 eV¹³. It is again the O1s and N1s in Figure S7d and Figure S7e shows similar features, which can confirms that the surface chemical composition of graphene *via* liquid phase exfoliation are similar; however, the contents are slightly different due to the lateral size. Note that the N1s spectra of a large graphene samples (942 nm-graphene) is quite board and noise, this is because the nitrogen species are typically functionalised at the edge atom of graphene (less nitrogen atom were found in the large graphene sample due to an unexfoliated effects).

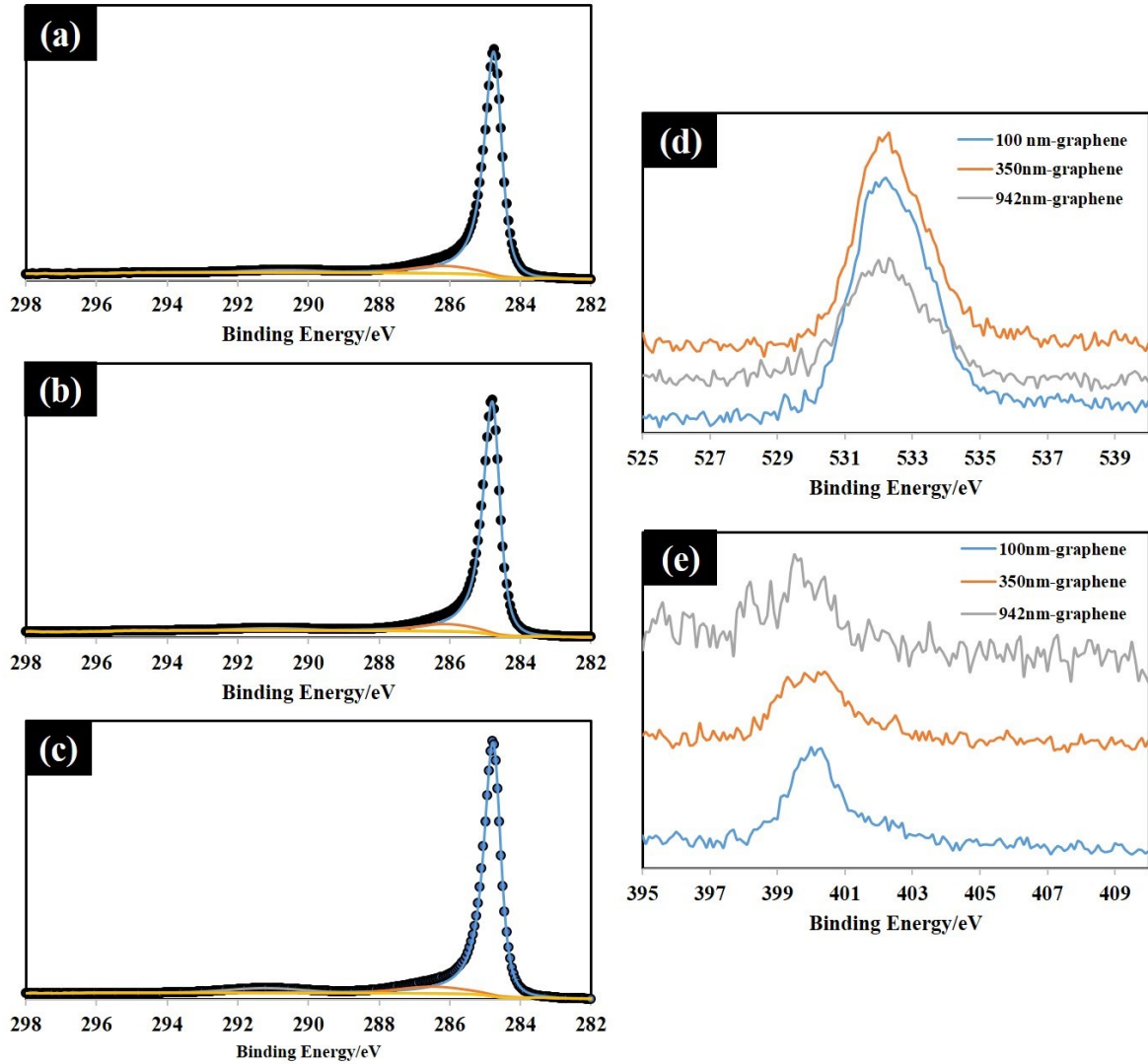


Figure S7: the high resolution XPS spectra of the as exfoliated graphene samples (a-c) C1s spectra of 100 nm to 942 nm graphene, (d) O1s spectra, and (e) N1s spectra.

Electrochemical properties of graphene

To obtain the capacitance shown in **Figure 3a**, the CV was applied to measure the electrochemical properties of the individual graphene flakes. It is clear that different graphene flake sizes show a unique electrochemical value, as shown in **Figure S8**. Overall, the 100 nm-graphene provides the highest specific current when compared to the 350 nm- and 942 nm-graphene. However, the CV of the 100 nm-graphene displays a distorted shape away from the ideal rectangular shape, indicating less conductive properties for this

material¹⁴ (see **Figure S8a**). This is due to the partial oxidation at the edge plane of the graphene during the sample preparation.¹⁵ The pseudocapacitive properties from the oxygen species is involved in the 100 nm-graphene sample,¹⁶ while the CV of 350-nm graphene exhibits a rectangular shape, indicating ideal supercapacitor behaviour (less oxygen species found on the sample).¹⁴ In contrast, the larger graphene flakes (942 nm-graphene) in **Figure S8c** shows poor electrochemical performance due to high resistivity and low capacitive properties when compared to those of 100 nm- and 350 nm-graphene. This is because the structural properties of 942 nm-graphene approach those of graphite. However, all samples reveal different EDLC properties which are shown in **Figure S8d**. The capacitance of all the graphene samples show an almost straight line when plotted against the scan rate (capacitance are less dependent on the scan rate). It was found that the capacitances of 100 nm-graphene are about 6.6, 6.6, 6.6, 6.4, 6.2 F g⁻¹ at the scan rates of 10, 25, 50, 75, 100 mV s⁻¹, respectively. For the 350 nm-graphene, the capacitances are about 3.5, 3.4, 3.4, 3.2, 3.0 F g⁻¹ when the scan rate is increased from 10 mV s⁻¹ to 100 mV s⁻¹. Again, the capacitance retention is unchanged for the 942 nm-graphene, showing a capacitance of 0.5 F g⁻¹ for all applied scan rates. This confirms the pseudocapacitive contribution from the oxygen species.

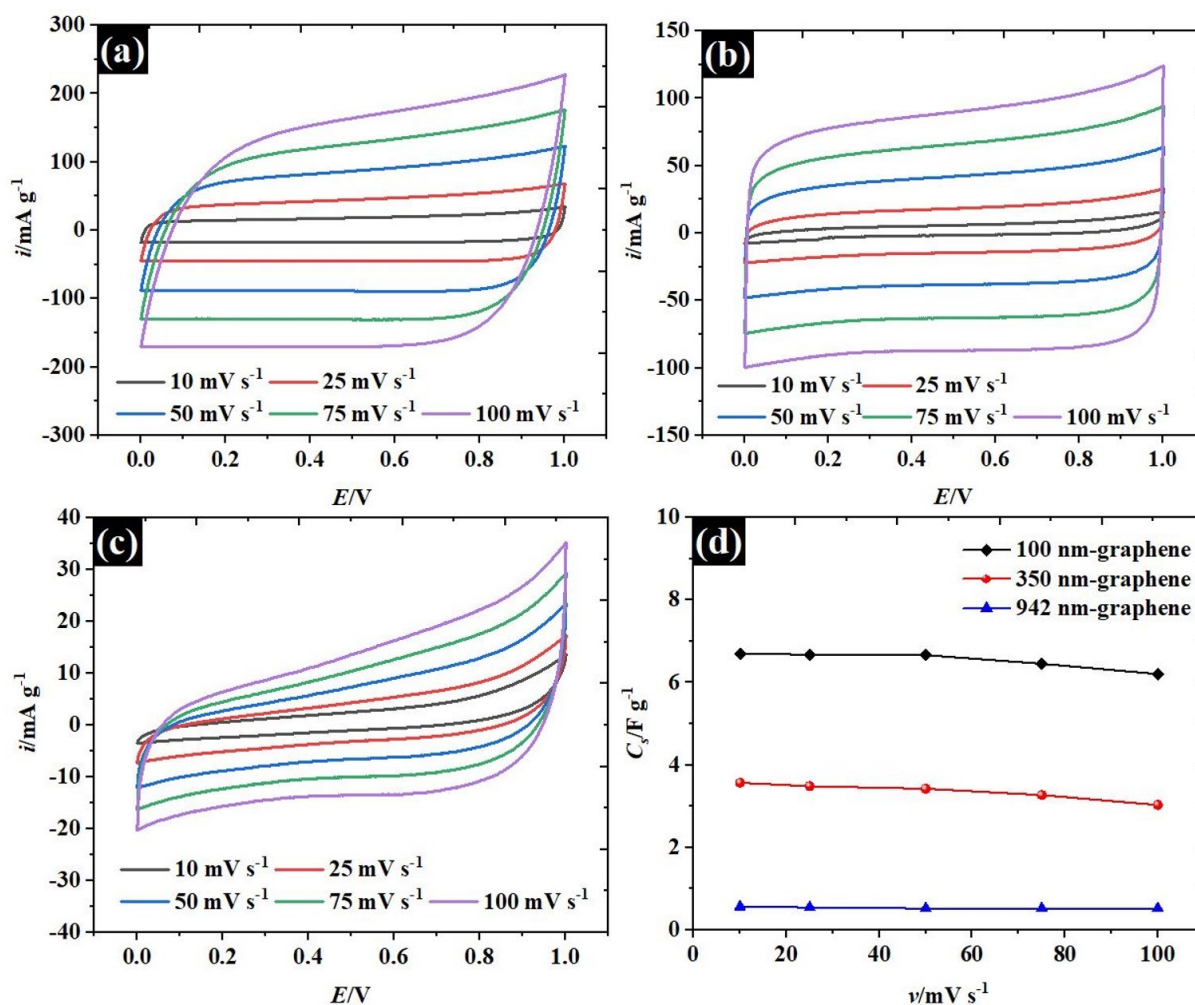


Figure S8: the CV of (a) 100 nm-graphene, (b) 350 nm-graphene, (c) 942 nm-graphene at different scan rates from 10 to 100 mV s^{-1} , and (d) the specific capacitance in relation to the scan rate.

Electrochemical properties of HOPG

To investigate the capacitance of basal plane graphitic carbon, the CV of the highly order pyrolytic graphite (HOPG) was carried out in saturated K_2SO_4 electrolyte (at a concentration of 0.69 M) as can be seen in **Figure S9**. It is evident that the CV of HOPG displays a potential window at between -0.5 and 0.6 V vs. Ag/AgCl. No reaction is found between -0.4 to 0.3 V vs. Ag/AgCl, confirming the EDLC properties. The positive branch of the CV was limited by the oxygen evolution reaction while the negative branch was limited by the oxygen reduction reaction.⁵ This potential window range agrees with the $C-E$ curve in **Figure 3b**.

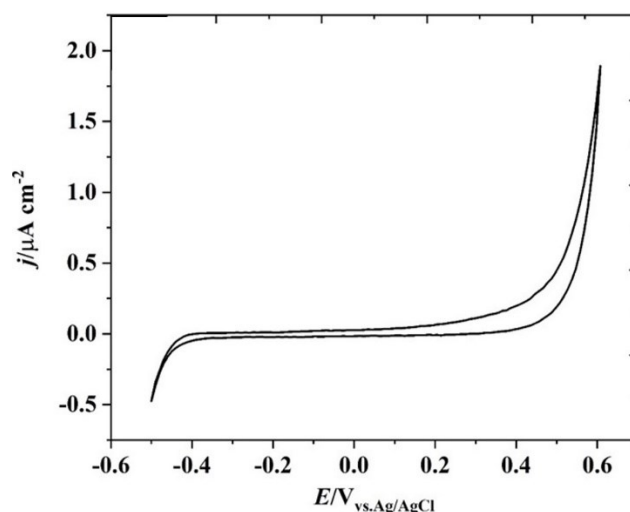


Figure S9: the CV of freshly cleaved basal plane HOPG at 100 mV s^{-1} in saturated K_2SO_4 solution (0.69 M concentration) over the potential window from -0.5 to 0.6 V vs. Ag/AgCl.

Impedance analysis

Table S1: the fitted parameters of all graphene samples

L/nm	R_{SM}/Ω	R_{HT}/Ω	R_{DBL}/Ω	C/ μF	Q/ μF	N	G/S cm^{-2}
942	123	39.3	71.6	60.4	10.2	1.00	5.61×10^{-3}
350	137	122	693	6.78	6.92	0.91	1.38×10^{-3}
100	226	718	5910	5.20	6.57	0.74	1.91×10^{-4}

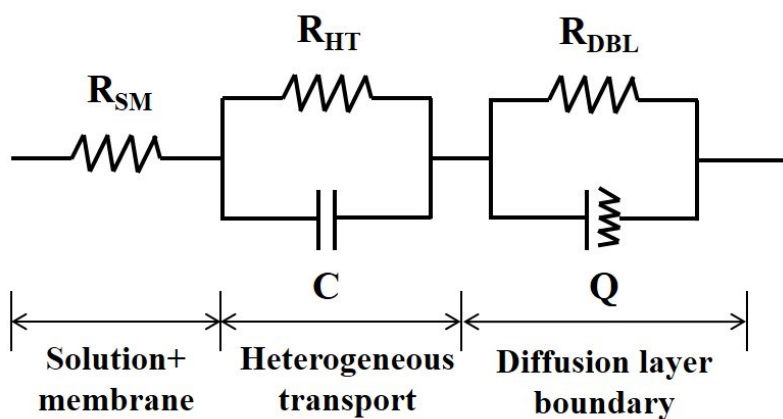


Figure S10: the equivalent circuit using four point probe measurement.

References

1. P. Iamprasertkun, W. Hirunpinyopas, A. M. Tripathi, M. A. Bissett and R. A. W. Dryfe, *Electrochimica Acta*, 2019, **307**, 176-187.
2. Y. Hernandez, V. Nicolosi, M. Lotya, F. M. Blighe, Z. Sun, S. De, I. T. McGovern, B. Holland, M. Byrne, Y. K. Gun'Ko, J. J. Boland, P. Niraj, G. Duesberg, S. Krishnamurthy, R. Goodhue, J. Hutchison, V. Scardaci, A. C. Ferrari and J. N. Coleman, *Nature Nanotechnology*, 2008, **3**, 563-568.
3. W. Hirunpinyopas, P. Iamprasertkun, M. A. Bissett and R. A. W. Dryfe, *Carbon*, 2020, **156**, 119-129.
4. P. Iamprasertkun, W. Hirunpinyopas, V. Deetrakul, M. Sawangphruk and C. Nualchimplee, *Nanoscale Advances*, 2020, DOI: 10.1039/D0NA00592D.
5. P. Iamprasertkun, A. Ejigu and R. A. W. Dryfe, *Chemical Science*, 2020, **11**, 6978-6989.
6. R. J. Good, *Journal of the American Chemical Society*, 1952, **74**, 5041-5042.
7. P. Iamprasertkun, W. Hirunpinyopas, A. Keerthi, B. Wang, B. Radha, M. A. Bissett and R. A. W. Dryfe, *The Journal of Physical Chemistry Letters*, 2019, **10**, 617-623.
8. M. J. McAllister, J.-L. Li, D. H. Adamson, H. C. Schniepp, A. A. Abdala, J. Liu, M. Herrera-Alonso, D. L. Milius, R. Car, R. K. Prud'homme and I. A. Aksay, *Chemistry of Materials*, 2007, **19**, 4396-4404.
9. S. S. Nemala, P. Kartikay, S. Prathapani, H. L. M. Bohm, P. Bhargava, S. Bohm and S. Mallick, *Journal of Colloid and Interface Science*, 2017, **499**, 9-16.
10. S. Sarkar, D. Gandla, Y. Venkatesh, P. R. Bangal, S. Ghosh, Y. Yang and S. Misra, *Physical Chemistry Chemical Physics*, 2016, **18**, 21278-21287.
11. M. A. Bissett, S. D. Worrall, I. A. Kinloch and R. A. W. Dryfe, *Electrochimica Acta*, 2016, **201**, 30-37.
12. Z. Li, L. Wang, D. Sun, Y. Zhang, B. Liu, Q. Hu and A. Zhou, *Materials Science and Engineering: B*, 2015, **191**, 33-40.
13. M. Lotya, Y. Hernandez, P. J. King, R. J. Smith, V. Nicolosi, L. S. Karlsson, F. M. Blighe, S. De, Z. Wang, I. T. McGovern, G. S. Duesberg and J. N. Coleman, *Journal of the American Chemical Society*, 2009, **131**, 3611-3620.
14. Y. Zhu, S. Murali, M. D. Stoller, K. J. Ganesh, W. Cai, P. J. Ferreira, A. Pirkle, R. M. Wallace, K. A. Cychoz, M. Thommes, D. Su, E. A. Stach and R. S. Ruoff, *Science*, 2011, **332**, 1537.
15. M. A. Bissett, I. A. Kinloch and R. A. W. Dryfe, *ACS Applied Materials & Interfaces*, 2015, **7**, 17388-17398.
16. C. Tan, X. Cao, X.-J. Wu, Q. He, J. Yang, X. Zhang, J. Chen, W. Zhao, S. Han, G.-H. Nam, M. Sindoro and H. Zhang, *Chemical Reviews*, 2017, **117**, 6225-6331.